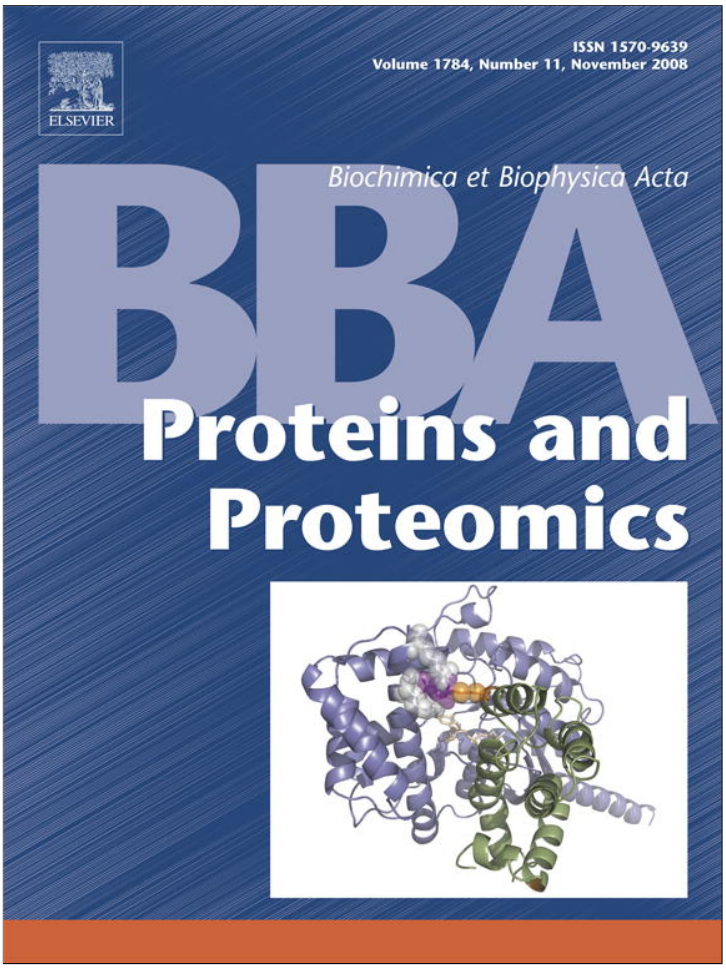

Biochimica et Biophysica Acta 1784 (2008) 1590–1595

Contents lists available at ScienceDirect

Biochimica et Biophysica Acta

journal homepage: www.elsevier.com/locate/bbapap

Structure of mistletoe lectin I from *Viscum album* in complex with the phytohormone zeatin

Arne Meyer [a], Wojciech Rypniewski [b], Maciej Szymański [b], Wolfgang Voelter [c], Jan Barciszewski [b], Christian Betzel [a,*]

[a] Institute of Biochemistry and Molecular Biology, University of Hamburg, c/o DESY, Notkestr. 85, Building 22a, 22603 Hamburg, Germany
[b] Institute of Bioorganic Chemistry of the Polish Academy of Sciences, Noskowskiego 12, 61-704 Poznan, Poland
[c] Institute of Physiological Chemistry, University of Tübingen, Hoppe-Seyler-Strasse 4, 72076 Tübingen, Germany

ARTICLE INFO

Article history:
Received 29 February 2008
Received in revised form 18 July 2008
Accepted 18 July 2008
Available online 31 July 2008

Keywords:
Cytokinin
Mistletoe lectin
Zeatin
Microgravity
Plant hormone
Water stress

ABSTRACT

The crystal structure of mistletoe lectin I (ML-I) isolated from the European mistletoe *Viscum album* in complex with the most active phytohormone zeatin has been analyzed and refined to 2.54 Å resolution. X-ray suitable crystals of ML-I were obtained by the counter-diffusion method using the Gel-Tube R crystallization kit (GT-R) onboard the Russian Service Module on the international space station ISS. High quality hexagonal bipyramidal crystals were grown during 3 months under microgravity conditions. Selected crystals were soaked in a saturated solution of zeatin and subsequently diffraction data were collected applying synchrotron radiation. A distinct F_o-F_c electron density has been found inside a binding pocket located in subunit B of ML-I and has been interpreted as a single zeatin molecule. The structure was refined to investigate the zeatin–ML-I interactions in detail. The results demonstrate the ability of mistletoe to protect itself from the host transpiration regulation by absorbing the most active host plant hormones as part of a defense mechanism.

1. Introduction

Cytokinins (CKs) are a group of phytohormones, first discovered during the 1950′s and characterized as substances able to induce plant cell division and differentiation. Most natural CKs are N6-substituted adenine derivatives generated as degradation products during depurination of DNA [1]. Since their discovery a substantial number of biochemical, physiological and genetic studies have focused on elucidating the diverse roles of CKs in plant growth and particular water transport and water stress conditions [2]. Cytokinins are also involved in other essential processes as sink/source relationship, vascular development, chloroplast differentiation, apical dominance and senescence. It seems that these effects result from molecular interactions with other plant hormones and environmental signals [3].

Zeatin, 6-(4-hydroxy-3-methylbut-2-enylamino)purine (Fig. 1), was found at first in maize and is the most common and most active CK identified so far [4]. Studies concerning structure–activity relationships have revealed the importance of the isoprenoid side chain for cytokinin activity [5]. Although the effects of cytokinins in plants are well known, the mechanism of their perception is still not fully understood [6,7]. Moreover, zeatin and other N6-substituted adenines show pharmacological activity in humans and found applications in molecular medicine [1].

Plant lectins are a heterologous group of proteins classified on the basis of their ability to bind in a reversible and specific way sugar molecules and more complex carbohydrates [8]. It is also known that plant lectins are directed against foreign glycans and accordingly they can interact with other organisms, either in recognition or even with defence related activities. In addition to the carbohydrate binding affinity a number of lectins have hydrophobic sites and binding pockets capable of accommodating distinct hydrophobic ligands [9,10]. The specific binding of non-carbohydrate ligands to lectins demonstrates the bifunctional nature of this protein family. Mistletoe lectin I (ML-I) is a member of the ribosome inactivating proteins type II (RIP type II) family. ML-I is a heterodimeric plant protein with a carbohydrate binding B-chain and an enzymatic A-chain. The latter acts on the ribosome and inhibits the protein synthesis by cleaving the *N*-C glycosylic bond of a specific adenine residue in the 28S rRNA. There are three structurally distinct types of RIPs: type I — simple polypeptide chain, type II — consisting of chain A, functionally equivalent to type I and a second B-chain with lectin function, and type III — a single chain with carboxy-terminal extension of unknown function [11,12]. The bipartite molecular structure of ML-I also facilitates its binding to the mammalian cell surface, to enter via endocytic uptake and to deliver the catalytically active polypeptide

* Corresponding author. Tel.: +49 40 8998 4744; fax: +49 40 8998 4747.
E-mail address: Betzel@unisgi1.desy.de (C. Betzel).

1570-9639/$ – see front matter © 2008 Elsevier B.V. All rights reserved.
doi:10.1016/j.bbapap.2008.07.010

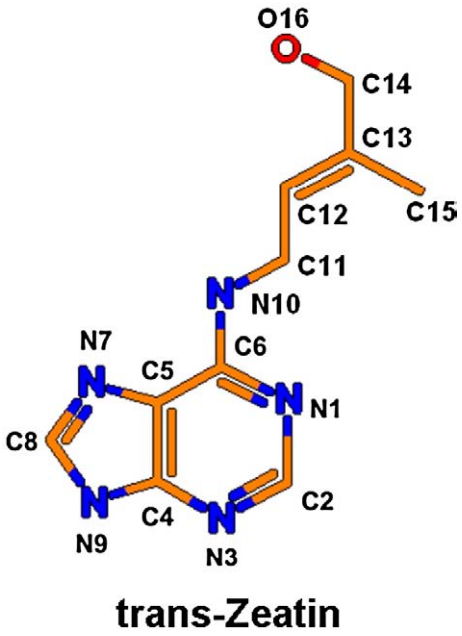

Fig. 1. Chemical structure of zeatin and atom nomenclature as used in the text.

into the cytoplasm, where it inhibits protein synthesis as described before [13]. To understand the regulatory potential of ML-I the structural analysis of complexes with plant hormones like cytokinins is of particular interest since these compounds occur naturally and perform regulatory functions in water transport and water stress response [14,15].

2. Material and methods

2.1. Protein purification

For protein isolation crude material of the European mistletoe (*Viscum album*) growing on apple trees (*Malus domestica*) was collected during February to March. After removal of fruits, leaves and small branches tissues were flash-frozen and ground into powder, dissolved in water and centrifuged. The supernatant was loaded on an affinity column with lactose immobilized with divinyl sulphone [16]. ML-I was purified and separated from other lectins by aminophenyl-boronic-acid affinity chromatography as described previously [17]. Prior to crystallization ML-I was dialyzed against 0.2 M glycine–HCl buffer at pH 2.5.

2.2. Crystallization

Crystals of ML-I were obtained applying the liquid phase counter-diffusion technique in the Granada Crystallization Box (GCB) using the Gel-Tube (GT-R) system [18] as shown in Fig. 2, with the following crystallization parameters and configuration specifications: the protein concentration was 5 mg/ml in 0.2 M glycine/HCl buffer, pH 2.5. 1.0 M ammonium sulphate in 0.2 M glycine/HCl buffer at pH 2.5 was used as precipitant. The capillary length was 75 mm with an inner diameter of 0.5 mm. The silicon gel-tube length was 15 mm after attachment to the capillary and the remaining gel length inside the silicon tube was 10 mm (Fig. 2). For the microgravity experiment six capillaries were used positioned in a single GCB set-up. The length of the precipitant solution was set to 66 mm, the protein solution length inside the capillary was adjusted to 55 mm. The experiment was performed at 20 °C. Hexagonal bipyramidal crystals of ML-I have been obtained after 109 days under microgravity conditions onboard the Russian Service Module on the ISS. The

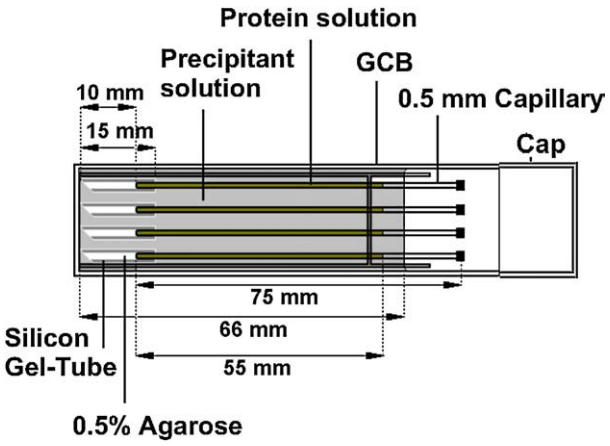

Fig. 2. Diagram illustrating the components and dimensions of the Granada Crystallization Box.

experiment was arranged by the Japanese Space Agency (JAXA), in terms of the JAXA GCF flight number 6. For data collection the crystals were retrieved from the capillaries and placed for 2 h in a saturated zeatin (Sigma-Aldrich, Z-3541, CAS-6025-53-2) soaking solution, containing 1.0 M ammonium sulphate in 0.2 M glycine/HCl, pH 2.5.

2.3. Data collection and processing

X-ray diffraction data were collected from a flash-frozen crystal at 100 K up to 2.54 Å resolution using a 165 mm MAR CCD detector at the consortium beam line X13 (HASYLAB/DESY). Prior to freezing crystals were soaked in a reservoir solution containing 20% v/v

Table 1
Details of data collection and refinement parameters

X-ray source	DESY, Hamburg, beam line X13
Temperature (K)	100
Resolution range (Å)	20.0–2.54 (2.59–2.54)[a]
Wavelength (Å)	0.8073
Space group	$P6_522$
Cell parameters: $a=b$, c (Å)	106.97, 312.36
No. observations	421,065
No. unique reflections	37,722
R_{merge} (%)[b]	6.4 (49)
Completeness (%)	99.5 (99.8)
$I/\sigma(I)$ in high-resolution bin	2.5
Mosaicity [°]	0.28
Data redundancy	3.5 (3.6)
Final R factor/R_{free} (%)	18.5/22.4
No. protein atoms	3965
No. solvent molecules	282
No. carbohydrate atoms	72
Other atoms	56
Average B factors (Å^2)	
Protein	45.6
Solvent	50.2
Ligand	47.9
Overall	45.9
R.m.s.d. from ideal bond length (Å)	0.018
R.m.s.d. from ideal bond angles (°)	1.84
Ramachandran plot, % residues in regions	
Most favored	88.7
Additionally allowed	10.4
Generously allowed	0.9
PDB ID	3D7W

[a] The figures in brackets are for the last resolution shell.
[b] $R_{merge}=\Sigma_{hkl}\ \Sigma_i|I_i\ (hkl)-\langle I(hkl)\rangle|\Sigma_{hkl}\ \Sigma_i\ I_i\ (hkl)$, where I_i (hkl) and $\langle I(hkl)\rangle$ are the observed individual and mean intensities of a reflection with the indices hkl, respectively, Σ_i is the sum over i measurements of a reflection with the indices hkl, and Σ_{hkl} is the sum over all reflections.

glycerol, saturated with zeatin. Data processing and data scaling were carried out using DENZO and SCALEPACK [19]. The crystals belong to the space group $P6_522$ with a single ML-I molecule in the asymmetric unit. Unit cell parameters were $a=b=106.97$ Å and $c=312.36$ Å. The packing parameter V_M was calculated to be 4.3 Å^3/Da [20], which corresponds to a solvent content of 71%. The data collection and scaling statistics are summarized in Table 1. Statistical parameters of crystals grown under microgravity have been evaluated and compared to their Earth-grown counterparts. As expected and shown in Fig. 3a and b, ML-I crystals grown in microgravity show clear tendencies of improved crystal quality in terms of lower mosaic spread [22–24]. A number of native ML-I crystals have been used for a comparative and statistical evaluation of the crystal quality (Fig. 3). Beside zeatin other plant hormones have been considered as possible ligands for ML-I and soaking experiments with ML-I crystals grown under microgravity have been carried out with olomoucine [25] and kinetin [1] as well. The resulting data sets were also used for the statistical evaluation and shown in Fig. 3a and b.

2.4. Refinement

The previously refined structure of the ML-I in complex with adenine (PDB ID: 1M2T) [26] was used as starting model for initial refinement applying the CCP4i program suite [27], after removing the solvent and ligand atoms. Model building and refinement was carried out applying the program REFMAC 5 [28,29] using all data up to 2.54 Å resolution. 5% of the reflections were excluded from the refinement and were used for the R_{free} statistics. Manual rebuilding and automatic real space positional refinement of the model and electron density interpretation based on the $2F_o$-F_c as well as the F_o-F_c electron density maps were done using the graphics program COOT [30], running on a Dell precision workstation 380. The zeatin molecule could be identified unambiguously using the F_o-F_c map contoured at 3σ level. The purin part of zeatin was refined at full occupancy. The O16 atom of the isoprenyl section of zeatin (Fig. 1) was positioned with 50% occupancy in corresponding *trans*- as well as in the *cis*-configuration. Both conformations are stabilized by an alternative network of H-bonds and solvent molecules, as shown in Fig. 5a and b. Solvent

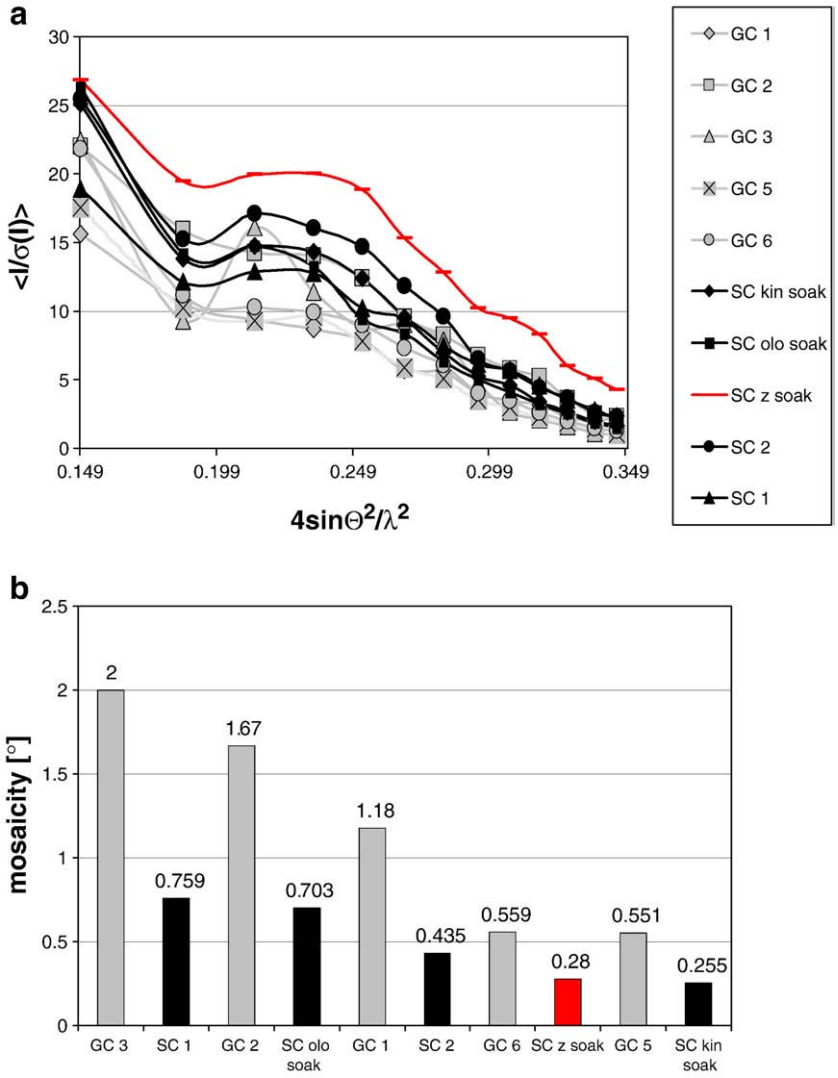

Fig. 3. (a) Signal-to-noise ratio vs. resolution of X-ray data collected from native ML-I crystals grown under 1 g conditions called Ground control (GC) in comparison to space grown crystals (Space crystals, SC) used for soaking experiments with different cytokinin plant hormones. The ML-I crystals (V_M=4.4 Å^3/Da) grown under microgravity indicate a higher quality in terms of intensities and therefore are more appropriate to be used for high-resolution data collection than their earth grown counterparts. Reflections of complete diffraction data sets has been used. (b) Comparative statistics for the mosaic spread of native ML-I crystals grown in space (SC) colored in black to ground control experiments (GC) colored in grey. Soaked crystals are labeled according to the compound applied for soaking, olo: olomoucine, z: zeatin, kin: kinetin. These mosaicity values did not have the Instrument Resolution Function smearing deconvoluted out, which would make the lower mosaicity values notably even smaller [21].

molecules were included with suitable hydrogen bonding partners, if observed as spherical peaks at a level of at least 2.5 σ in the F_o-F_c difference electron density. ML-I is known to have four potential NAG *N*-glycosylation sites, characterized by sequence motifs Asn-X-Ser/Thr [31]. The sites are located at Asn 112 in subunit A and Asn 308, Asn 343 and Asn 383 in subunit B. In the course of the refinement, F_o-F_c maps showed carbohydrate densities at all four glycosylation sites. However, only one NAG residue could be identified at Asn 112 and at Asn 308, while two NAG residues were visible at the other two sites. The refinement was terminated when no further significant improvement could be archived in the *R*-factor statistics, model completeness, Ramachandran statistics and electron density. The final *R* value for the ML-I zeatin complex was 18.5% and R_{free} was 22.4% for all data between 20.0 and 2.54 Å resolution. The program PROCHECK was applied to validate the quality of the final structure [32]. 88.7% of the residues were found in the most favored regions of the Ramachandran plot, 10.4% were located in additional allowed regions and 0.9% of residues were in the generously allowed regions. Details of the refinement statistics are summarized in Table 1. Deviations from the ideal geometry are found for residues Ala 223 of subunit A and residues Asn 487 and Ser 489 of subunit B. All are located on flexible surface loops.

3. Results and discussion

3.1. Statistical diffraction data evaluation

The application of microgravity conditions and the environment on the International Space Station (ISS) for protein crystal growth has been described in detail before [33,34]. We used the advantages of microgravity to grow crystal of ML-I in terms of the JAXA GCF flight number 6 applying the Granada crystallization box (Fig. 1). ML-I crystals have a relative high solvent content of approx. 75% and crystal growth of ML-I is known to benefit from space environment [26]. The obtained ML-I crystals were analyzed together with the ground grown counterparts applying synchrotron radiation. Data collection parameters were kept identical. The signal to noise ratio and the mosaicity was compared versus resolution. A clear tendency towards lower mosaicity and better signal/noise ratio has been observed for the space grown crystals. A brief summary of the statistical evaluation is shown in Fig. 3a and b. In an earlier ML-I crystallization experiment under microgravity conditions onboard the ISS, using the high density protein crystal growth system on the international space station mission ISS 6A [26], we could obtain high quality crystals and could collect a data set for a ML-I adenine complex up to 1.9 Å resolution at the wiggler beam line BW7B at DESY/EMBL Hamburg applying a MAR 345 IP detector. A direct comparison is not advisable as the diffraction data we describe here were collected on a bending magnet beam with different optics and CCD detector.

3.2. Overall crystal structure and model quality

The refined overall X-ray structure consists of ML-I complexed with a single zeatin molecule, one sulphate ion, four glycerol molecules as well as 282 solvent molecules in the asymmetric unit. The ML-I model consists of 510 amino acid residues in two subunits (subunit A, 1–248 and subunit B, 249–510) and 6 glycan residues located at four glycosylation sites. The overall structure is shown in Fig. 4. According to the commonly accepted nomenclature of RIP II proteins, and a homologous structure of ricin [35], subunit A is subdivided in three domains. Domain I includes amino acid residues 1–109, which form four central strands βd, βe, βf and βg in antiparallel orientation, flanked by a long and a short alpha helix, αA and αB. The two beta strand pairs βa–βd and βg–βh at the two edges are almost parallel. Domain II (residues 110–198) consists predominantly of α-helices. The helices αC, αD and αE are bundled in

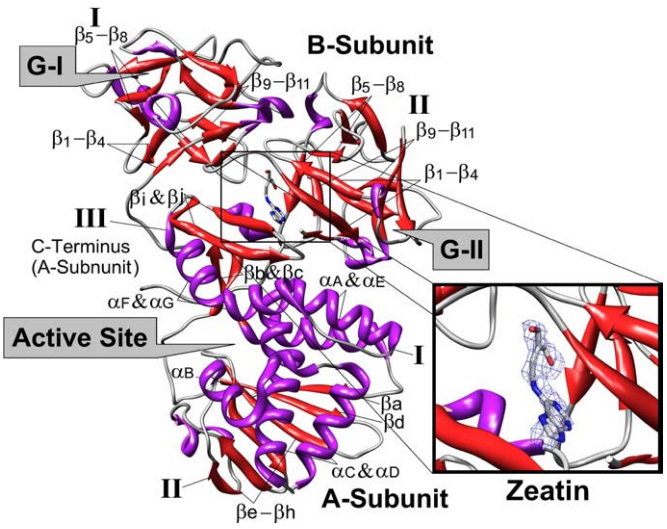

Fig. 4. Cartoon plot of mistletoe lectin I in complex with zeatin. Subunit B is shown on the top and subunit A below. The zoomed zeatin binding cavity is located almost at the center of the protein. The bound zeatin molecule is shown in stick mode. Galactose binding sites are indicated as G-I and G-II. The active site region is indicated as well. Magnification of bonded zeatin shows an $2F_o$-F_c-Signal contoured at 1.5 σ. Domains are indicated by latin numbers.

a cluster enclosed by the beta sheet of Domain I. Domain III (residues 199–248) includes helix G and interacts with subunit B through the antiparallel β-sheet strands βi and βj. A single disulfide bond between Cys 247 (A) and Cys 252 (B) connects both subunits covalently. In the present structure the last five C-terminal residues of the subunit A could not be modeled due to high flexibility. A structural feature of the A-subunit is the absence of internal disulfide bonds, allowing biological activity in the cytosolic environment.

Subunit B consists of two globular domains similar to those reported for ricin [36], presumably a result of gene duplication. Both domains consist of 12 antiparallel beta-sheets bundled into three clusters and stabilized by three internal disulfide bonds (Cys 311–Cys 328, Cys 399–Cys 412, and Cys 438–Cys 455). The two galactose-specific binding sites in subunit B are formed by different sets of residues [37].

3.3. Active site

The active site residues in chain A are Tyr 76, Tyr 115, Glu 165 and Arg 168 and are found in homologous positions in other RIP type proteins [38]. Other essential residues in the active site cleft are Asn 74, Arg 125, Gln 161, Glu 196 and Trp 199 [26]. The natural substrate adenosine binds with its aromatic group in a sandwich type stacking interaction between Tyr 76 and Tyr 115. Therefore, both phenyl groups of the tyrosines are found for the ML-I zeatin structure in a native parallel orientation. A single glycerol molecule of the cryo-protectant is found in the vicinity of the active site region.

3.4. Zeatin binding

A single zeatin molecule has been identified in a hydrophobic cavity, which is located in a region between the two globular domains of subunit B [10]. The total calculated volume of the cleft is approx. 1260 Å^3. Zeatin binds in the center of the cavity with the purine pointing towards the entrance. Zeatin is well coordinated by a number of hydrophobic and H-bond interactions shown in Fig. 5a and b. Residues of subunit A which are involved in zeatin binding are: Val 228 and Thr 229. These residues are located at βj of domain III; the binding residues Arg 234 and Asp 235 are located also in domain III at a rigid segment with almost α-helical geometry. This segment is found in similar orientation in other type II RIPs like ricin, ebulin I and

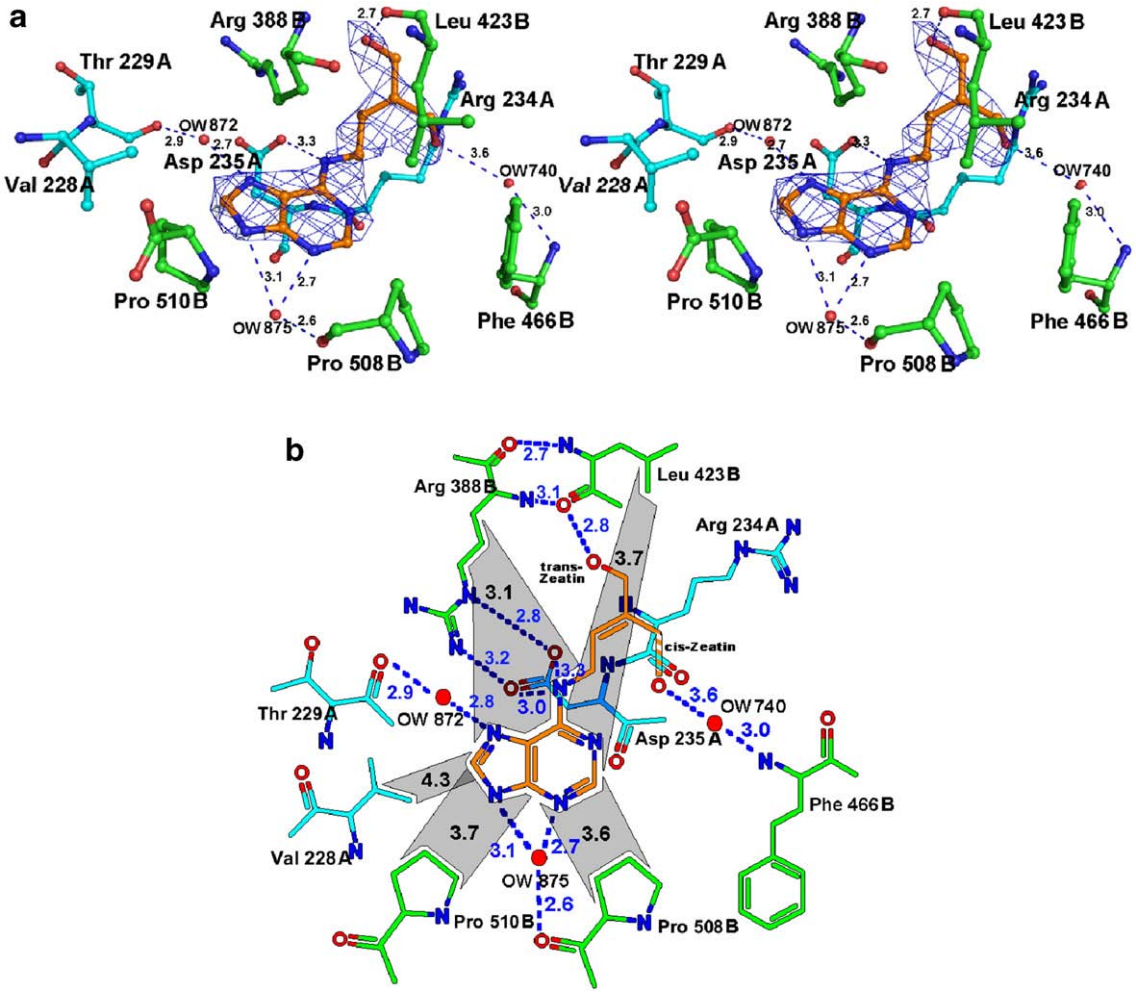

Fig. 5. (a) Stereoview showing zeatin and the interacting residues of ML-I. A-chain residues are colored turquoise and B-chain residues are colored green. Hydrogen bonds are shown as dashed lines. The corresponding F_o-F_c-electron density map of zeatin is shown in blue, contoured at 3.7 σ. (b) 2D scheme of showing all interactions of zeatin. Hydrophobic interactions are indicated as grey areas, hydrogen bonds in dashed blue lines.

abrin A. In subunit B zeatin binding is supported by the following residues of domain II: Leu 423, Pro 508 and Pro 510. Several solvent water molecules form H-bonds from ML-I to zeatin, as for example OW 872 from the carbonyl oxygen of Thr 229 to N7 of zeatin (Fig. 5b). The isoprenoide moiety of zeatin is stabilized via a hydrogen bond between N10 and the carboxyl group of Asp 235. The double conformation of the O16, which is confirmed by the omit map (Fig. 5a), supports the idea that the isoprenoide chain is found with equal occupancy in *trans*- as well as in *cis*-configuration. In *trans*-configuration the O16 atom has a H-bond to the carbonyl oxygen of Leu 423 whereas the *cis*-configuration is considered to be bridged to the main chain nitrogen of Phe 466 by a weak H-bond to OW 740 as shown in Fig. 5a and b. The binding of zeatin does not affect the overall structure of ML-I. A least square minimized superposition of ML-I complexed on zeatin with ML-I in a complex with adenine [26] gave an r.m.s. deviation for all Cα atoms of 0.39 Å. The major differences in Cα atom deviations up to 2.3 Å occur at two loop regions on the surface of the protein. A comparison of the zeatin binding region with both structures of ML-I shows clearly that binding of zeatin does not show any induced fit. Superposition of the residues that contribute to binding of zeatin (Fig. 5a and b) shows an r.m.s. value for all side chain atoms of 0.36 Å. In the ML-I adenine complex the position of the zeatin isoprenoide moiety is occupied by a single water molecule and a glycerol molecule. Initial calorimetric measurements (ITC) of the free binding enthalpy indicate that the binding constant is in the mM range, which corresponds to the observed binding and interactions shown in Fig. 5a and b.

4. Discussion

The crystal structure of ML-I reveals a cavity which accommodates zeatin specifically. No complexes were observed for the two structurally related plant hormones olomoucine and kinetin for which identical soaking experiments were carried out. Significant conformational changes of ML-I beyond the thermal displacement were not observed clarifying that an induced fit was not required to bind zeatin. The mistletoe accumulates substances transported by the host xylem-tissue primary to supply its own metabolism with required compounds from the host plant. Among these substances are the host hormones. Considering that mistletoe has an up to 7.5 fold higher transpiration rate than the host plant [39,40], tapping the xylem tissue of the host by mistletoe and the resulting additional substantial water consumption of mistletoe raises a water stress in the host and a deficit of those branches, which are above the mistletoe. As a consequence the host control systems for transpiration and functioning under stress respond to cope with the water stress situation. In order to increase the water transport from the roots the water potential in shoots and leaves needs to be decreased. One host response is a zeatin disbursement along the xylem-tissue axis that triggers the stomata opening [41–43]. As a result the water potential

decreases and the water delivery rate goes up. However, it has been shown that even at high level of phytohormones the transpiration of mistletoe leaves remains unaffected [44]. This supports the idea, that mistletoe has the ability to protect itself from the regulation of the host transpiration by absorbing and neutralizing zeatin and other phytohormones. It seems that in a course of the evolution the mistletoe developed a complex system of defensive functions. For ML-I the galactose-specific sugar binding sites in combination with the active site are covering the main ribosome inhibiting activity and provide defensive core capabilities against foreign hostile organisms. In addition to these defensive core activities ML-I has a specific capability to diminish its sensitivity to the host hormone level and therefore is capable to adapt as parasite.

5. Conclusion

Based on the statistical evaluation of the diffraction data sets, microgravity provides a useful environment to enhance crystal quality. Even after mechanical disturbance the space grown ML-I crystals show remarkably better diffraction properties in terms of signal to noise ratio and mosaicity then their ground grown counterparts. Those conditions have been exploited to obtain high quality data of a complex of the ribosome inactivating protein type II ML-I with the cytokinin zeatin. The X-ray structure has revealed a distinct single binding site within the two subunits, almost opposite to the active site region and the two galactose binding sites. Zeatin is part of the hormone regulatory system among some putative hosts for the mistletoe and interference with the mistletoe metabolism is intimated. The X-ray structure of a complex of ML-I with a hormone of the ubiquist cytokinin family is a clear indication that parasite host interactions have a biochemical and structural background that is yet not well understood.

Acknowledgements

The work was supported by grants from the Deutsche Luft- und Raumfahrtagentur (DLR under Project number: 50WB0615) and by the Polish Ministry of Higher Education and Science.

References

[1] J. Barciszewski, F. Massino, B.F. Clark, Kinetin a multiactive molecule, Int. J. Biol. Macromol. 40 (2007) 182–192.
[2] J. Pospisilova, H. Synkova, J. Rulcova, Cytokinins and water stress, Biol. Plantarum 43 (2000) 321–328.
[3] D.W. Mok, M.C. Mok, Cytokinin metabolism and action, Ann. Rev. Plant Physiol. Plant Mol. Biol. 89 (2001) 89–118.
[4] K. Takei, T. Tomoyuki, H. Sakakibara, Arabidopsis CYP735A1 and CYP735A2 encode cytokinin hydroxylases that catalyze the biosynthesis of *trans*-zeatin, J. Biol. Chem. 279 (2004) 41866–41872.
[5] F. Skoog, D.J. Armstrong, Cytokinin, Annu. Rev. Plant Physiol. 21 (1970) 359–384.
[6] B. Chow, P. McCourt, Plant hormone receptors: perception is everything, Genes Dev. 20 (2006) 1998–2008.
[7] C.E. Hutchinson, J. Li, C. Argueso, M. Gonzalez, E. Lee, M.W. Lewis, B.B. Maxwel, T.D. Perdue, G.E. Schalle, J.M. Alomso, J.R. Ecker, J.J. Kieber, The *Arabidopsis* histidine phosphotransfer proteins are redundant positive regulators of cytokinin signaling, Plant Cell 18 (2006) 3073–3087.
[8] E.J. Van Damme, A. Barre, P. Rouge, W.J. Peumans, Cytoplasmic/nuclear plant lectins: a new story, Trends Plant Sci. 9 (2004) 484–489.
[9] E.J. Zaluzec, M.M. Zaluzec, K.W. Olsen, S.F. Pavkovic, Crystallization and preliminary X-ray analysis of peanut agglutinin–N^6-benzylaminopurine complex, J. Mol. Biol. 219 (1991) 151–153.
[10] A. Meyer, W. Rypniewski, L. Celewicz, V.A. Erdmann, W. Voelter, T.P. Singh, N. Genov, J. Barciszewski, Ch. Betzel, The mistletoe lectin I–phloretamide structure reveals a new function of plant lectins, Biochem. Biophys. Res. Commun. 364 (2007) 195–200.
[11] S.W. Park, R. Vepachedu, N. Sharma, J.M. Vivanco, Ribosome-inactivating proteins in plant biology, Planta 219 (2004) 1093–1096.
[12] M. Ambrosi, N.R. Cameron, B.G. Davis, Lectins: tools for the molecular understanding of the glycocode, Org. Biomol. Chem. 3 (2005) 1593–1608.
[13] J.M. Lord, L.M. Roberts, J.D. Robertus, Ricin: structure, mode and action, and some current applications, FASEB J. 8 (1994) 201–208.
[14] N. Raman, S. Ehumaki, Presence of cytokinin in root nodules of *Casuarina equisetifolia*, I. J. Exp. Biol. 34 (1996) 577–579.
[15] B.J. Taller, Cytokinins and legume nodulation, Department of Biology, Memphis State University, Memphis, TN 38152, USA 55–59.
[16] S. Crider-Pirkle, P. Billingsley, C. Faust, D.M. Hardy, V. Lee, H. Weitlauf, Cubilin, a binding partner for galectin-3 in the murine utero–placental complex, J. Biol. Chem. 277 (2002) 15904–15912.
[17] Y. Li, U. Pfuller, E.L. Larsson, H. Jungvid, I.Y. Galaev, B. Mattiasson, Separation of mistletoe lectins based on the degree of glycosylation using boronate affinity chromatography, J. Chromatogr. 925 (2001) 115–121.
[18] H. Tanaka, K. Inaka, S. Sugiyama, S. Takahashi, S. Sano, M. Sato, S. Yoshitomi, A simplified counter diffusion method combined with a 1D simulation program for optimizing crystallization conditions, J. Synchr. Rad. 11 (2004) 45–48.
[19] Z. Otwinowski, W. Minor, Processing of X-ray diffraction data collected in oscillation mode, in: C.W. Carter Jr., R.M. Sweet (Eds.), Methods in Enzymology, Macromol. Crystallogr., vol. 276, Academic Press, New York, 1997, pp. 307–326.
[20] B.W. Matthews, Solvent content of protein crystals, J. Mol. Biol. 33 (1968) 491–497.
[21] M. Colapietro, G. Cappuccio, C. Marciante, A. Pifferi, R. Spagna, J.R. Helliwell, The X-ray diffraction station at the ADONE Wiggler facility: hardware, software and preliminary results (including crystal perfection), J. Appl. Cryst. 25 (1992) 192–194.
[22] N. Wakayama, D.C. Yin, K. Harata, T. Kiyoshi, M. Fujiwara, Y. Tanimoto, Macromolecular crystallization in microgravity generated by a superconducting magnet, Ann. N.Y. Acad. Sci. 1077 (2006) 184–193.
[23] A. Vegara, B. Lober, C. Sauter, R. Giege, A. Zagari, Lessons from crystals grown in the Advanced Protein Crystallisation Facility for conventional crystallisation applied to structural biology, Biophys. Chem. 118 (2005) 102–112.
[24] R.A. Judge, E.H. Snell, M.J. van der Woerd, Extracting trends from two decades of microgravity macromolecular history, Acta Cryst. D 61 (2005) 763–771.
[25] C.M. Crews, R. Mohan, Small-molecule inhibitors of the cell cycle, Curr. Opinion in Chem. Biol. 4 (2000) 47–53.
[26] R. Krauspenhaar, W. Rypniewski, N. Kalkura, K. Moore, L. DeLucas, S. Stoeva, A. Mikhailov, W. Voelter, Ch. Betzel, Crystallisation under microgravity of mistletoe lectin I from *Viscum album* with adenine monophosphate and the crystal structure at 1.9 Å resolution, Acta Cryst. D 58 (2002) 1704–1707.
[27] E. Potterton, P. Briggs, M. Turkenburg, E. Dodson, A graphical user interface to the CCP4 program suite, Acta Cryst. D 59 (2003) 1131–1137.
[28] Collaborative Computational Project, Number 4, Acta Cryst. D 50 (1994) 760.
[29] A.A. Vagin, R.A. Steiner, A.A. Lebedev, L. Potterton, S. McNicholas, F. Long, G.N. Murshudov, Refmac5 dictionary: organization of prior chemical knowledge and guidelines for its use, Acta Cryst. 60 (2004) 2184–2195.
[30] P. Emsley, K. Cowtan, Coot: model-building tools for molecular graphics, Acta Cryst. D 60 (2004) 2126–2132.
[31] W. Voelter, R. Wacker, S. Stoeva, R. Tsitsilonis, Ch. Betzel, Mistletoe lectins, structure and function, Front. Nat. Pro. Chem. 1 (2005) 149–162.
[32] R.A. Laskowski, M.W. MacArthur, D.S. Moss, J.M. Thornton, Procheck: a program to check the stereochemical quality of protein structures, J. Appl. Cryst. 26 (1993) 283–291.
[33] K. Jules, K. McPherson, K. Hrovat, E. Kelly, Initial characterization of the microgravity environment of the international space station: increments 2 through 4, Acta Astronaut. 55 (2004) 855–887.
[34] E.H. Snell, J.R. Helliwell, Macromolecular crystallization in microgravity, Rep. Prog. Phys. 68 (2005) 799–853.
[35] W. Montfort, J.E. Villafranca, A.F. Monzingo, S.R. Ernst, B. Katzin, E. Rutenber, N.H. Xoung, R. Hamlin, J.D. Robertus, The three-dimensional structure of Ricin at 2.8 Å, J. Biol. Chem. 262 (1987) 5398–5403.
[36] J.E. Villafranca, J.D. Robertus, Ricin B chain is a product of gene duplication, J. Biol. Chem. 256 (1981) 554–556.
[37] R. Mikeska, R. Wacker, R. Arni, T.P. Singh, A. Mikhailov, A. Gabdoulkhakov, W. Voelter, Ch. Betzel, Mistletoe lectin I in complex with galactose and lactose reveals distinct sugar-binding properties, Acta Cryst. F61 (2005) 17–25.
[38] B.J. Katzin, E.J. Collins, J.D. Robertus, Structure of ricin A-chain at 2.5 A, Proteins Struct. Funct. Genet. 10 (1991) 251–259.
[39] J.T. Fisher, Water relations of mistletoes and their hosts, in: M. Calder, P. Bernhardt (Eds.), The Biology of Mistletoes, Acad. Press, Sydney, 1983, pp. 161–184.
[40] I. Ullmann, L.O. Lange, H. Ziegler, J. Ehleringer, E.D. Schulze, I.R. Cowan, Diurnal courses of leaf conductance and transpiration of mistletoes and their hosts in central Australia, Oecologia 67 (1985) 577–587.
[41] F. Tardieu, W.J. Davies, Stomatal responses to abscisic acid is a function of current plant water status, Plant Physiol. 98 (1992) 540–545.
[42] F. Tardieu, J. Zhang, N. Katerji, O. Bethenod, S. Palmer, W.J. Davies, Xylem ABA controls the stomatal conductance of field-grown maize subjected to soil compaction or soil drying, Plant, Cell Environ. 15 (1992) 185–191.
[43] L.D. Incoll, P.C. Jewer, Cytokinins and stomata, in: E. Zeiger, G.D. Farquhar, I.R. Cowan (Eds.), Stomatal Function, Stanford University Press, Stanford, 1987, pp. 281–292.
[44] P. Escher, A.D. Peuke, P. Bannister, S. Fink, W. Hartung, F. Jiang, H. Rennenberg, Transpiration, CO_2 assimilation WUE, and stomatal aperture in leaves of *Viscum album* (L.): effect of abscisic acid (ABA) in the xylem sap of its host (*Populus x euamericana*), Plant Physiol. Biochem. 46 (2008) 64–70.